

HIGH-AMPLITUDE WALL PRESSURE EVENTS AND THEIR RELATION TO TURBULENT STRUCTURE IN CHANNEL FLOW

Ali Mehrez

Department of Energy Engineering and Science
Nagoya University
Chikusa-ku, Furo-cho, 464-8603, Japan
mehrez.ali.abdelmotaal.elsaid@f.mbox.nagoya-u.ac.jp

Tatsuya Tsuneyoshi

Department of Energy Engineering and Science
Nagoya University
Chikusa-ku, Furo-cho, 464-8603, Japan
t-tsuneyoshi@energy.nagoya-u.ac.jp

Yoshinobu Yamamoto

Department of Mechanical Systems Engineering
University of Yamanashi
Takeda, Kofu, Yamanashi, 400-8510, Japan
yamamotoy@yamanashi.ac.jp

Yoshiyuki Tsuji

Department of Energy Engineering and Science
Nagoya University
Chikusa-ku, Furo-cho, 464-8603, Japan
c42406a@nucc.cc.nagoya-u.ac.jp

ABSTRACT

Direct Numerical Data (DNS) set of fully developed turbulent channel flow is utilized to study the turbulent structures associated with positive and negative High Amplitude Pressure Peaks (HAPPKs) at different Reynolds number. Conditional average is conducted based on the wall pressure extrema that exceed a certain threshold value. The results indicate near-wall shear layer in the buffer zone, and the large-scale streamwise velocity upstream the detection point together contribute to average positive pressure. Upon splitting the total pressure to its slow and rapid parts, the contribution from the rapid part, that represents the effect of large-scale motion, is dominant throughout the channel except close to the wall which its comparable with slow part. Hence, positive HAPPKs result from both small- and large- scale structures. Negative peaks are found to be associated with the core of the vortex structure. The conditional averaged Q-value introduced an organized vortex structure that scale with wall units with negative peak coincides with its core, and hence negative peaks are generated from the small-scale motion. The effect of Reynolds number appears only in the positive peaks.

INTRODUCTION

The generation of pressure fluctuations inside turbulent boundary layer is connected to the dynamics of the velocity fluctuations linearly, via the interaction between the velocity fluctuations and the mean shear, and nonlinearly via the interaction of velocity fluctuations with themselves. Among the pressure fluctuations, wall pressure fluctuations had been studied extensively due to the difficulty inherent in measuring the fluctuations of pressure inside the boundary layer.

High Amplitude Pressure Peaks (HAPPKs) refer to both positive and negative pressure fluctuations that exceed a threshold value k larger than the root mean square (r.m.s) value p_{rms} . These HAPPKs are the main responsible for the sound generation that

often lead to undesirable structural vibrations. Starting with analysis of Kim (1981) with variable-interval space averaging (VISA) detection method, he found that bursting phenomenon is associated with a pressure signature characterized by a positive peak surrounded by small negative amplitude regions.

Later, Johansson et al. (1987) concluded that buffer region shear layer structures are responsible for the generation of positive peaks. As the wall pressure fluctuations are generated from linear and nonlinear interactions, they suggested that positive HAPPKs are generated from the interaction with the mean shear which were supported by Johanson et al. (1991) in their study of shear layer structures. On the other hand, negative peaks were conjectured to be associated with sweep type events.

Robinson (1991) claimed that negative pressure troughs beneath the extended vortex leg, while positive pressure is located along the high-low speed interface of the near wall shear layers that seem to extended to the wall. This near wall shear layers are created when high-speed fluid impacts low-speed fluid lifted by quasistreamwise vortices. Moreover, Kim et al. (2002) suggested that positive peaks are associated with the inward motion because of the streamwise vortices above the wall, whereas high negative wall pressure occur beneath the outward motion in the vicinity of the wall.

The analysis of Ghaemi and Scarano (2013) led them to the conclusion that positive HAPPK region is overlapping with the shear layer structure, in agreement with Johansson et al. (1987), where interaction between upstream sweep events, initiated from the outer layer, and downstream ejection ones, formed by the hairpin category in the inner layer, forms the shear layer. In agreement with Robinson (1991), they related the negative pressure to the core of the vortical structures which could be either spanwise or streamwise section of a hairpin vortex, or it may be associated with an isolated streamwise vortex.

It is apparent from these and other studies that the various coupling mechanisms between flow structures in both the inner and the outer layers of the boundary layer, and wall pressure

fluctuations peaks are quite complex. In addition, the work of Ghaemi and Scarano (2013) was handled at relatively moderate Reynolds number, $Re_\tau = 770$ based on friction velocity u_τ and kinematic viscosity ν . Consequently, it is not clear if these structures depend on Reynolds number or not. DNS data set of fully developed turbulent channel flow covers a wide range of Reynolds number, from $Re_\tau = 180$ to 4000, $Re_\tau = u_\tau h / \nu$, where h is channel half width, are used for firstly, studying the turbulence structures concerned with both positive and negative HAPPKs, and secondly, to check their universality with Reynolds number. The abstract is organized as follows. In section II, an overview of the utilized DNS data set is introduced. Section III will be concerned with discussion of the results the conditional average analysis of positive and negative HAPPKs. Finally, the conclusion will be given in Section V.

NUMERICAL SIMULATION

The simulations reported in this study are DNSs of incompressible turbulent flow between two parallel planes. The coordinate system is taken to be (x, y, z) that are representing the streamwise, wall-normal, and spanwise coordinates, respectively with $u_i = (u_1, u_2, u_3) = (u, v, w), i = 1, 2, 3$ are the three components of velocity in the same directions. For the pressure, p is used to denote the total pressure. In streamwise (x) and spanwise (z) directions, periodic boundary conditions are applied, and no-slip/no-penetration boundary conditions are applied at the wall. The mass flux through the channel remains constant by a uniform streamwise pressure gradient that drives the flow field.

DNSs of the incompressible Navier–Stokes equation are conducted by a hybrid Fourier spectral (x, z) and the second-order central difference method in (y) direction, where aliasing error in the streamwise and spanwise directions is removed by the phase shift method. For time progress, third-order accuracy Runge-Kutta method is applied to the convection term, Crank-Nicolson method is applied to the viscosity term, and the Euler implicit method is applied to the pressure term. The present DNS conditions are shown in Table 1. The domain size is relatively large to detect the large-scale structures exist around the center of the channel. The time taken for a hypothesized turbulent eddy to perform one complete 360° rotation and, known as eddy turn over time T^* , is given also in Table 1.

Table 1 illustrates the computational domain size in streamwise and spanwise directions (L_x, L_z), in addition to the grid resolutions in the three directions ($\Delta x^+, \Delta y^+, \Delta z^+$), where Δy_w^+ represents the grid resolution at the wall, and Δy_c^+ is at the center of the channel. Table 1 gives the number of grid points in N_y , the wall-normal direction.

STATISTICAL ANALYSIS

Statistical Features of Pressure Fluctuations

The data to be presented will show that the probability distribution of the amplitudes has features obviously different

from the Gaussian signal. In comparison to the Gaussian distribution, the wall pressure fluctuations have larger positive and negative amplitudes as illustrated in Figure 1. A comparison of the higher moments of the probability distribution between the present data and the Gaussian distribution illustrates this distinction. Table 2 gives the values of the skewness, as a measure of the asymmetry behavior of the probability distribution, and the kurtosis, as a measure of the intermittent character, of wall pressure in comparison with the previous study of Schew (1983) for turbulent boundary layer at $Re_\tau = 1400$, based on the momentum thickness of the boundary layer. We compare the results of Schew (1983) with the smallest transducer d^* comparable with the grid spacing in the streamwise direction Δx^+ . In addition, we compare our results for the higher Reynolds number with the successful experimental study of Tsuji et al. (2007).

The flatness factor value shows the intermittent feature of the wall pressure as it takes a value of ≈ 5.5 irrespective of Reynolds number, but the results of Tsuji et al. (2007) shows a monotonic decreasing with the Reynolds number. On the other hand, the skewness factor shows slight increase with Reynolds number. In addition, it takes positive value for the higher Reynolds numbers of 2000 and 4000 in agreement with the results of Tsuji et al. (2007).

Figure 2 shows the contribution of the HAPPKs to the total r.m.s of wall pressure fluctuations at different k values. The contributions were determined by computing the r.m.s values from all events that exceeded the current threshold. Obviously, the data show large amplitude events more than 3 threshold value contribute to nearly 40.7% of the total r.m.s of pressure fluctuations which coincides with the results of Schew (1983).

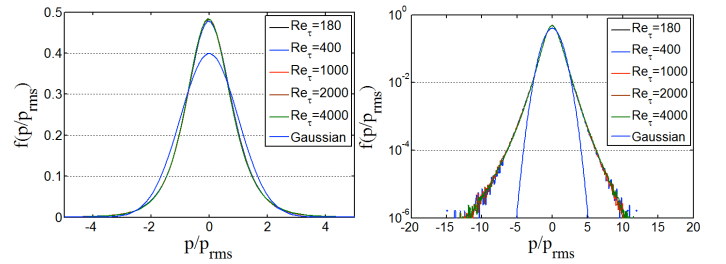


Figure 1. Probability Density Distribution (pdf) of wall pressure fluctuations for Reynolds number range in Table 1 in (a) linear, and (b) logarithmic scale

Table 1. Calculation conditions for DNS data set

Re_τ	$\frac{L_x}{h}$	$\frac{L_z}{h}$	Δx^+	Δz^+	Δy_w^+	Δy_c^+	N_y	$\frac{T^*}{Re_\tau}$
180	12.8	6.4	12.0	7.2	0.3	3.8	192	12.4
400	12.8	6.4	13.3	6.7	0.17	4.3	384	10.4
1000	12.8	6.4	13.3	8.3	0.6	8.0	512	11.2
2000	16.0	6.4	16.0	8.3	0.6	8.0	1024	13.3

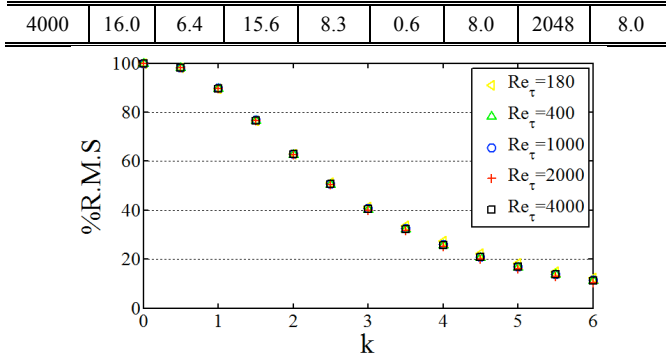


Figure 2. Relative contributions to the total r.m.s of wall pressure fluctuations at different threshold values

Table 2. Higher moments for the present DNS data set and the previous studies

	$\Delta x^+ / d^+$	Re_τ / Re_θ	Skewness	kurtosis
Present	$\Delta x^+ = 12.0$	$Re_\tau = 180$	-0.08	5.73
Present	$\Delta x^+ = 13.3$	$Re_\tau = 400$	-0.03	5.49
Present	$\Delta x^+ = 13.3$	$Re_\tau = 1000$	-0.001	5.57
Present	$\Delta x^+ = 16.0$	$Re_\tau = 2000$	0.02	5.57
Present	$\Delta x^+ = 15.6$	$Re_\tau = 4000$	0.07	5.57
Schew (1983)	$d^+ = 19$	$Re_\theta = 1400$	-0.18	4.9
Tsuji et al. (2007)	$d^+ = 4.6$	$Re_\theta = 5870$	-0.05	5.2
Tsuji et al. (2007)	$d^+ = 14.5$	$Re_\theta = 16700$	0.09	4.5

Conditional Averaging

Conditional sampling technique is utilized to detect the coherent turbulent structures associated with positive and negative HAPPKs. The sampling is computed when the wall-pressure fluctuation exceeds a certain value over its local r.m.s value. Local extrema (maxima and minima) of wall pressure are detected and then the quantity M is averaged over a volume of (aa, bb, cc) in streamwise, wall-normal and spanwise directions, respectively. The center of this volume is the extreme wall pressure located at (x_{ex}, z_{ex}) with extension bb in the wall-normal direction. Johansson et al. (1991) indicated that instantaneous shear layer structures often tend to develop asymmetries while propagating downstream. The shear is generated from the interaction of high- and low-speed regions through a localized spanwise motion that results in a spanwise gradient of the streamwise velocity at the center of the shear layer. Therefore, the conditional sampling is based on another constraint, beside the pressure, depending on the positive or the negative slope of the streamwise velocity at the center position of the volume. The threshold value of $k = 3$ is used as introduced in Figure 2.

RESULTS AND DISCUSSION

Positive HAPPKs

Starting with the conditional averaging results of the positive HAPPKs, Figure 3 illustrates the averaged velocity field in the conditional domain around the positive point at $Re_\tau = 180$. The

velocity patterns indicate the positive pressure is related to strong shear layers in the buffer layer, as it is clearly noted in the average field in $x-z$ plane in Figure 6 at $y^+ = 15$. Both the high streamwise velocity region accompanied with downward flow to the vicinity of the wall in the upstream side (sweep events), and the negative- u in conjunction with positive- v (ejection events) downstream the detection point, give rise to the formation of the shear layer inclined with around 45° with respect to x . A near-wall shear layer is formed due to the re-direction of the high-speed fluid impacting the upstream face of the low-speed fluid. This creates a quasi-stagnation zone which results in a positive HAPPK. This agrees with results of Johansson et al. (1987), Johansson et al. (1991) and Ghaemi and Scarano (2013). The origin of the sweep events seems to be beyond the inner layer as they exceed $y^+ = 100$, while the ejection events appear to be induced close to the wall as noted in Figure 5 for the contour lines in $x-y$ plane. Unlike the streamwise velocity, wall-normal velocity contours show slice decrease with Reynolds number in outer scaling. Also, the iso-surface of the streamwise velocity around the detection point shown in Figure 4 illustrates this structure.

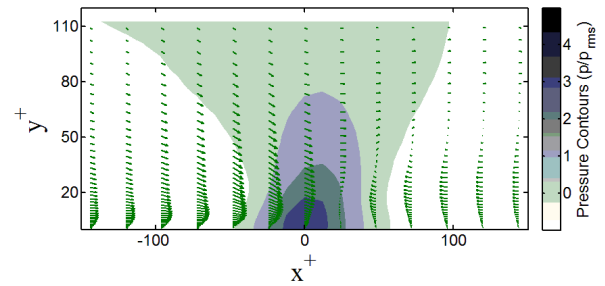


Figure 3. Velocity field in the mid $x-y$ plane with the pressure contours normalized with their local r.m.s value at $Re_\tau = 180$

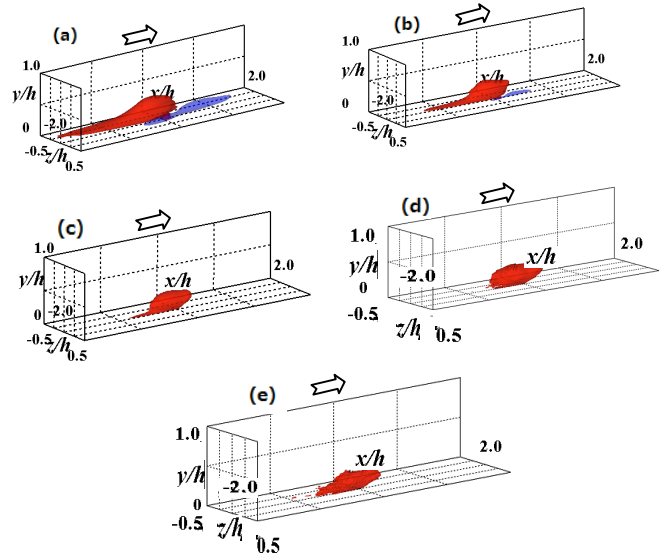


Figure 4. Iso-surfaces streamwise velocity (outer scaling), $u^+ = 1$ (red) and $u^+ = -1$ (blue) at (a) $Re_\tau = 180$, (b) $Re_\tau = 400$,

(c) $Re_\tau = 1000$,(d) $Re_\tau = 2000$,(e) $Re_\tau = 4000$. The arrow indicates the direction of the flow.

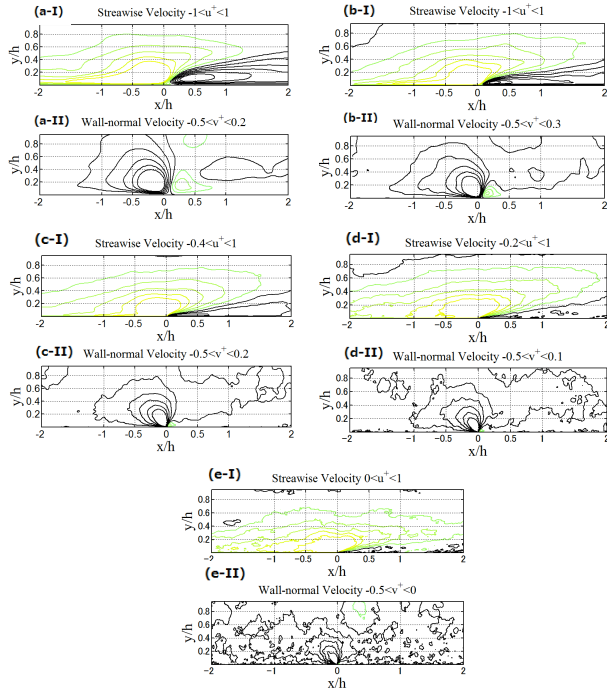


Figure 5. streamwise and wall-normal velocity contours (outer scaling) in the mid $x - y$ plane at (a) $Re_\tau = 180$, (b) $Re_\tau = 400$, (c) $Re_\tau = 1000$,(d) $Re_\tau = 2000$,(e) $Re_\tau = 4000$ (black lines illustrate negative contours).

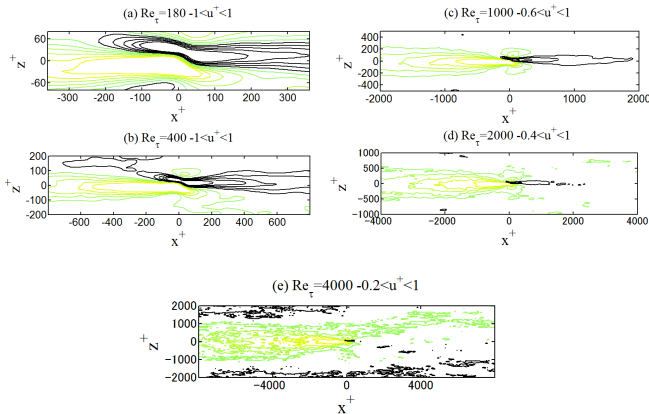


Figure 6. streamwise velocity contours in $x - z$ plane at $y^+ = 15$ (inner scaling) at (f) $Re_\tau = 180$, (f) $Re_\tau = 400$, (g) $Re_\tau = 1000$,(h) $Re_\tau = 2000$,(i) $Re_\tau = 4000$.

From the above it can be observed that large-scale structures in the outer region have contributions to the formation of the near-wall shear layer via sweep events. R.M.S wall pressure scaled with mixed variables; friction velocity u_τ and channel mean centerline velocity U_0 (Tsuji et al, 2007), infers that wall pressure is affected by fluid structures in the inner and outer layer. This suggests that these large-scale structures affect the

wall pressure directly, and affect it also indirectly through the near-wall shear layer.

An attempt to quantify this behaviour may be introduced by splitting the pressure into slow and rapid parts as introduced by Kim (1989). The conditionally averaged slow and rapid pressure fields around the positive point for the different Reynolds number are shown in Figure 7 to analyze the scale separation that contributes to the increase in the wall pressure. The inner scaling of the coordinates indicates that the slow pressure shows strong positive correlation up to around $y^+ \approx 100$, while the rapid pressure extends its positive correlation to the channel center independently of Reynolds number. This is consistent with the direct footprint of the large-scale structures of the outer layer upon the positive pressure peak that appears clearly in the rapid part. In a more detailed view, the contribution to the averaged pressure field from the slow and rapid parts along the channel is given in Figure 8 in both linear and logarithmic scales. Near the wall, both parts contribute equally to the averaged total pressure up to around $y^+ = 10$. With increasing Reynolds number, the contribution from the slow part in the vicinity to the wall increase. However, getting away from the wall, the contribution is more from the rapid part. Accordingly, the positive HAPPK results from the large-scale structure in the outer layer, and from the near-wall shear layer in the buffer zone.

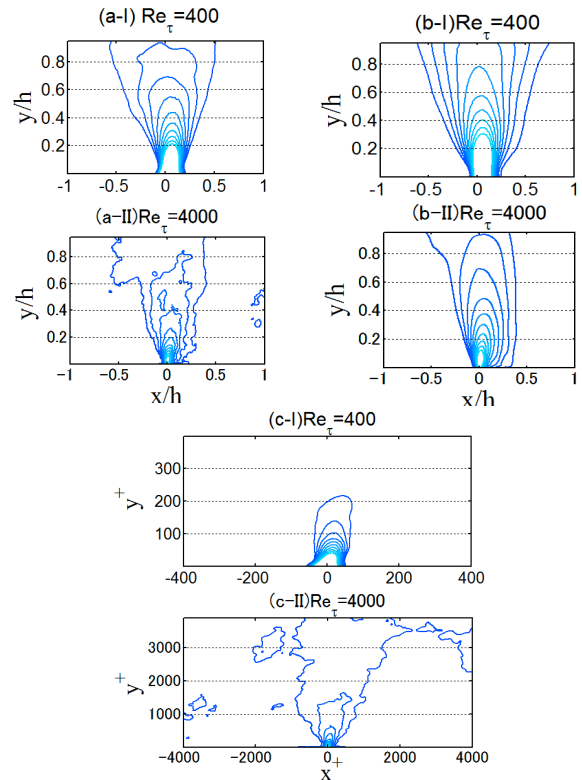


Figure 7. (a) Total (outer scaling), (b) rapid (outer scaling), and (c) slow (inner scaling) pressure positive contours normalized with their local r.m.s value, at $Re_\tau = 400$ and $Re_\tau = 4000$. Contour lines are from 0.1 to 1.

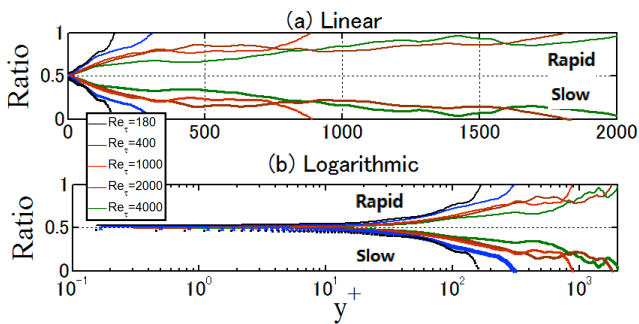


Figure 8. Averaged slow (blue) and rapid (black) pressure contributions in (a) linear and (b) logarithmic scales at $Re_\tau = 180$ to $Re_\tau = 4000$ (symbols represent the slow part).

Negative HAPPKs

The positive pressure is found to be associated with the shear layer with sweep events originate from the outer layer in addition to the direct contribution from the outer layer. As stated previously, negative HAPPKs were subjected to many conjectures throughout the literature. Contrary to the positive pressure peaks which observed to be surrounded with the vortex field (not shown here), negative pressure shows loopy structures that is overlapping the vortex structure. This is indicated in the snapshot realization in Figure 9 for the iso-surfaces of the vortex structures computed by Q-criterion. Accordingly, it is suggested that there is a correlation between the negative pressure cluctaitions and the vortex field highly populated in the vicinity of the wall.

From the instantaneous realization, it can be inferred that negative pressure is associated with different types of the vortical structures. Figure 10 illustartes three different vortical shapes that inhabit vicinity to the wall. Negative pressure is clearly overlaps the head and the neck of the hairpin vortex in Figure (10-a), and the cores of the spanwise and the quasi-streamwise vortices in Figure (10-b) and (10-c), respectively. The neagive pressure is found to be connected to their cores. Figure 11 indicates the iso-surfaces, normalized in wall units, for the averaged vortex field around the negative HAPPKs and visulaized in inner scaling coordinates. The negative HAPPKs was found to be consistent with the core of the resultatnt vortex structure that result from conditionally averaging over different shapes of the vortex structures. The resultant vortex structure is scaled with the wall units and doesn't show Reynolds number dependence. It is to be thought that negative pressure regions are generated by the small scale vortex structure saced with wall units. Accordingly, they may not be influenced by the large scale structure appears at higher Reynolds number.

Unlike the results of Ghaemi and Scarano (2013) who obtained a clear hairpin vortex structure with a negative pressure point within its head, the current study doesn't introduce such organized structure, alternatively an ellepsoid structures is extracted. This may be attributed to the different vortical sstructures exist within the turbulent boundaty layer, with quasi-streamwise vortices are the most inhabitants in the near-wall

layer, as stated by Robinson (1991). In addition, as the Reynolds number increases the frequency of occurrence of the hairpin vortex decreases. Ghaemi and Scarano (2013) may separate the different stuctures and then conducted the conditional average, but their study doesn't refer to such separation.

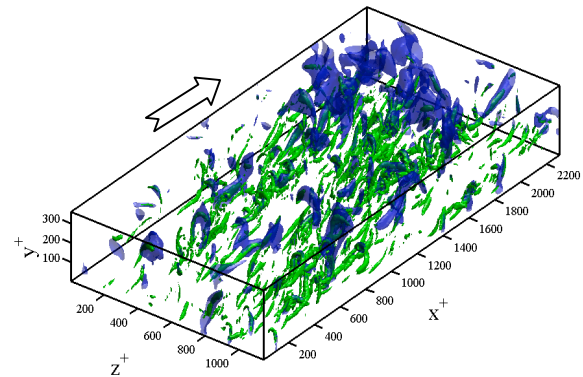


Figure 9. Instantaneous iso-surfaces of pressure (transparent blue) at $p/p_{rms} = -2$ and vortex struture (solid green) at $Q^* = 0.02$ at $Re_\tau = 180$. The arrow indicates the direction of the flow.

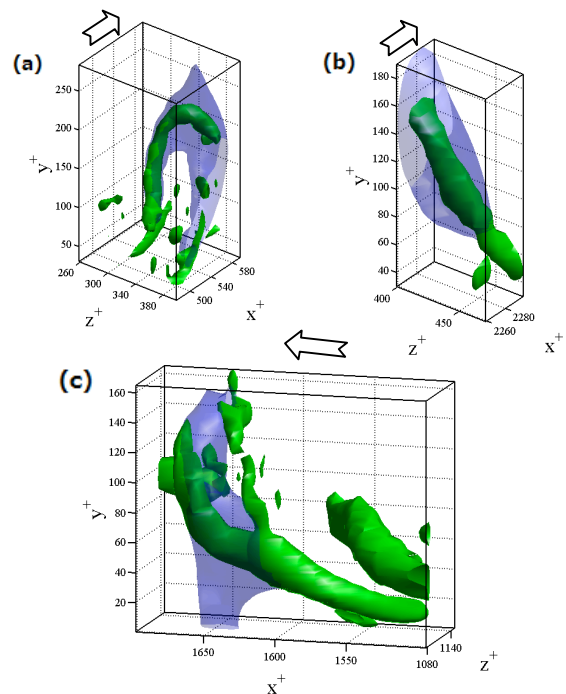


Figure 10. Instantaneous iso-surfaces of pressure (transparent blue) at $p/p_{rms} = -2$ and (a) hairpin vortex (solid green), (b) spanwise vortex (solid green), and (c) quasi-streamwise vortex (solid green) at $Q^* = 0.02$ at $Re_\tau = 180$. The arrow indicates the direction of the flow.

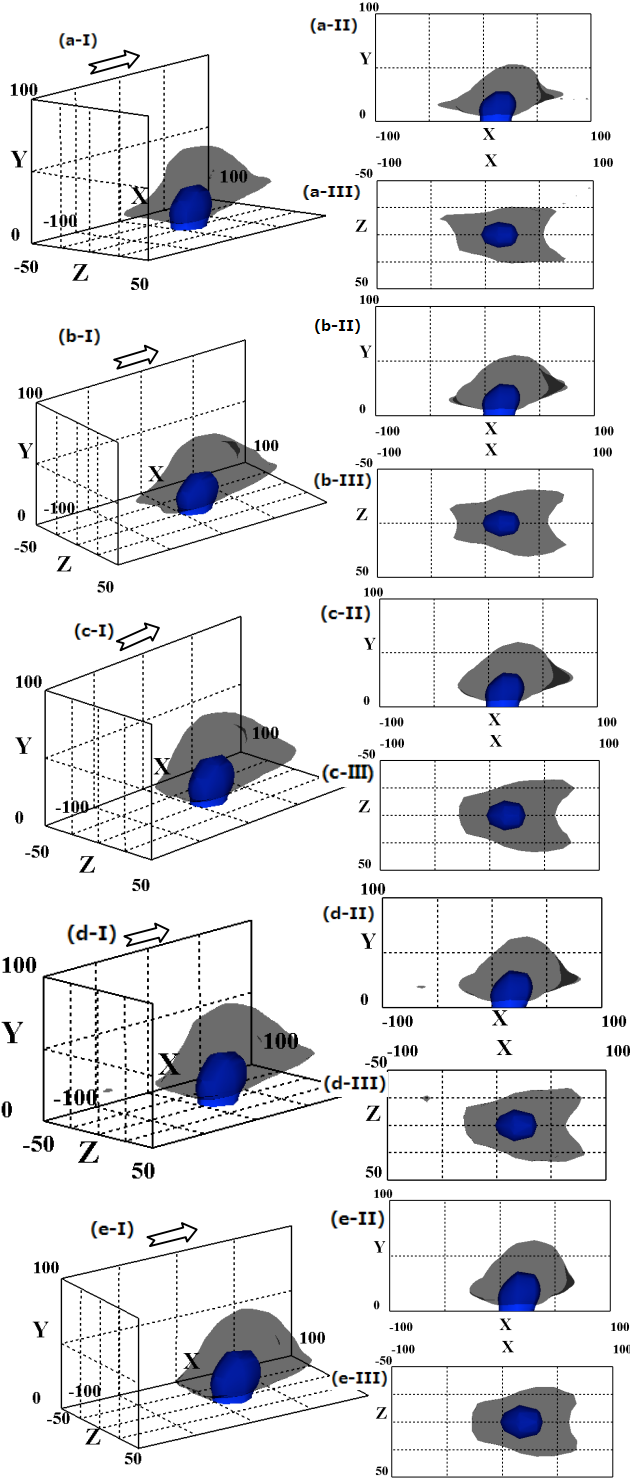


Figure 11. Isosurface of conditionally average pressure fluctuations $p/p_{rms} = -3$ (solid blue) and vortex organization $Q^+ = 0.002$ (transparent black). (i) Three-dimensional view, (ii) $x-y$ plane, and (iii) $x-z$ at (a) $Re_\tau = 180$, (b) $Re_\tau = 400$, (c) $Re_\tau = 1000$, (d) $Re_\tau = 2000$, (e) $Re_\tau = 4000$. The arrow indicates the direction of the flow. In this figure $X \equiv X^+$, $Y \equiv Y^+$, and $Z \equiv Z^+$.

CONCLUSION

In this abstract, we introduce the analysis of coherent structures associated with positive and negative HAPPKs from DNSs data set covers a wide range of Reynolds number from $Re_\tau = 180$ to $Re_\tau = 4000$. Positive HAPPKs are found to result from both the near-wall shear layer in the buffer zone, and from large-scale structures that are normalized with the outer scaling. Also, these large scale-structures contribute to the formation of the shear-layer via sweep events upstream the positive detection point. Negative HAPPKs result from the small-scale vortex structures in the near-wall region. The averaged results introduce organized structures from different vortex structures with the negative pressure peaks coincide with the core of the vortex. The conditioned Q-value shows Reynolds number independence. Finally, it should be noted that these results are based on the conditional average analysis which may not introduce an actual portrayal of the physical domain.

ACKNOWLEDGEMENT

This research used computational resources of the K-computer provided by the RIKEN Advanced Institute for Computational Science through the HPCI System Research project (Project ID:hp140196), and is partially supported by "Joint Usage/Research Center for Interdisciplinary Large-scale Information Infrastructures" in Japan (Project ID:jhl60045-MDJ). Thanks are due to Mr. Masayuki Sano for his valuable help.

REFERENCES

- Ghaemi, S., and Scarano, F., 2013, "Turbulent Structures of High-Amplitude Pressure Peaks within TheTurbulent Boundary Layer", *J. Fluid Mech.*, Vol. 735, pp. 381-426.
- Johansson, A. V., Her, J. Y., and Haritonidis, J. H., 1987, "On The Generation of high-amplitude Wall-Pressure Peaks in Turbulent Boundary Layers and Spots", *J. Fluid Mech.*, Vol. 175, pp. 119-142.
- Johansson, A. V., Alfredsson, P. H., and Kim, J., 1991, "Evolution and Dynamics of Shear-Layer Structures in Near-Wall Turbulence", *J. Fluid Mech.*, Vol. 224, pp. 579-599.
- Kim, J., 1989, "On The Structure of Pressure Fluctuations in Simulated Turbulent Channel Flow", *J. Fluid Mech.*, Vol. 205, pp. 421-451.
- Kim, J., 1983, "Turbulent Structures associated with The Bursting Event", *Physics of Fluids*, Vol. 28, pp. 52-58.
- Kim, J., Choi, J., and Sung, H. J., 2002, "Relationship between Wall-Pressure Fluctuations and Streamwise Vortices in a Turbulent Boundary Layer", *Phys. of Fluids*, Vol. 14, pp. 898-901.
- Robinson, S. K., 1991, *The Kinematics of Turbulent Boundary Layer Structures*, Ph.D. Thesis, Stanford University, Stanford.
- Schew, G., 1983, "On the Structure and Resolution of Wall-Pressure Fluctuations associated with Turbulent Boundary Layer Flow", *J. Fluid Mech.*, Vol. 134, pp. 311-328.
- Tsuji, Y., Fransson, J. H. M., Alfredsson P. H., and Johansson, A. V., 2007, "Pressure Statistics and Their Scaling in

High-Reynolds-Number Turbulent Boundary Layers”, *J. Fluid Mech.*, Vol. 585, pp. 1–40.